



HAL
open science

Phosphatidylglycerol::Prolipoprotein Diacylglyceryl Transferase (Lgt) of Escherichia coli Has Seven Transmembrane Segments, and Its Essential Residues Are Embedded in the Membrane

Jérémy Pailler, Willy Aucher, Magali Pires, Nienke Buddelmeijer

► **To cite this version:**

Jérémy Pailler, Willy Aucher, Magali Pires, Nienke Buddelmeijer. Phosphatidylglycerol::Prolipoprotein Diacylglyceryl Transferase (Lgt) of Escherichia coli Has Seven Transmembrane Segments, and Its Essential Residues Are Embedded in the Membrane. *Journal of Bacteriology*, 2012, 194 (9), pp.2142 - 2151. 10.1128/JB.06641-11 . pasteur-01407680

HAL Id: pasteur-01407680

<https://pasteur.hal.science/pasteur-01407680>

Submitted on 2 Dec 2016

HAL is a multi-disciplinary open access archive for the deposit and dissemination of scientific research documents, whether they are published or not. The documents may come from teaching and research institutions in France or abroad, or from public or private research centers.

L'archive ouverte pluridisciplinaire **HAL**, est destinée au dépôt et à la diffusion de documents scientifiques de niveau recherche, publiés ou non, émanant des établissements d'enseignement et de recherche français ou étrangers, des laboratoires publics ou privés.

Phosphatidylglycerol::Prolipoprotein Diacylglyceryl Transferase (Lgt) of *Escherichia coli* Has Seven Transmembrane Segments, and Its Essential Residues Are Embedded in the Membrane

Jérémy Pailler,^{a,b} Willy Aucher,^a Magali Pires,^a and Nienke Buddelmeijer^a

Institut Pasteur, Unité Génétique Moléculaire, CNRS ERL 3526, Paris, France,^a and Université Paris Diderot, Sorbonne Paris Cité, Unité Génétique Moléculaire, Paris, France^b

Lgt of *Escherichia coli* catalyzes the transfer of an *sn*-1,2-diacylglyceryl group from phosphatidylglycerol to prolipoproteins. The enzyme is essential for growth, as demonstrated here by the analysis of an *lgt* depletion strain. Cell fractionation demonstrated that Lgt is an inner membrane protein. Its membrane topology was determined by fusing Lgt to β -galactosidase and alkaline phosphatase and by substituted cysteine accessibility method (SCAM) studies. The data show that Lgt is embedded in the membrane by seven transmembrane segments, that its N terminus faces the periplasm, and that its C terminus faces the cytoplasm. Highly conserved amino acids in Lgt of both Gram-negative and Gram-positive bacteria were identified. Lgt enzymes are characterized by a so-called Lgt signature motif in which four residues are invariant. Ten conserved residues were replaced with alanine, and the activity of these Lgt variants was analyzed by their ability to complement the *lgt* depletion strain. Residues Y26, N146, and G154 are absolutely required for Lgt function, and R143, E151, R239, and E243 are important. The results demonstrate that the majority of the essential residues of Lgt are located in the membrane and that the Lgt signature motif faces the periplasm.

Bacterial lipoproteins are characterized by their fatty-acylated amino termini via which they are anchored into lipid membranes. They have a wide variety of biological functions in bacteria, such as maintenance of cell envelope architecture (Lpp and Pal) (7, 8), insertion and stabilization of outer membrane proteins (BamB) (40), uptake of nutrients and metals (OppA and SitC) (28), protein folding (PrsA) (24), bacteriocin release (BRP) (42), and adhesion and invasion (OspC and Lmb) (31) (for a recent review, see reference 29). Lipoproteins, which constitute 2 to 3% of bacterial proteomes, are synthesized in the cytoplasm as prolipoproteins and contain a conserved lipoprotein signature motif called lipobox [L(A/V)⁻⁴-L⁻³-A(S)⁻²-G(A)⁻¹-C⁺¹] that allows recognition by the lipoprotein modification machinery. (The invariant cysteine +1 becomes the first amino acid of the mature protein after modification; residues -4 to -1 are cleaved off as part of the signal peptide.) Lipoproteins are inserted into the membrane via the Sec or Tat secretion machinery (52, 53) and are modified on the outer leaflet of the (inner) membrane by the sequential action of three membrane-bound enzymes (Fig. 1). The first step is catalyzed by phosphatidylglycerol::prolipoprotein diacylglyceryl transferase (Lgt) that adds an *sn*-1,2-diacylglyceryl group, derived from phosphatidylglycerol, to the SH group of cysteine⁺¹, resulting in the formation of a thioether-linked diacylglyceryl-prolipoprotein and glycerolphosphate as a by-product (48). The second step is catalyzed by signal peptidase II (Lsp) that cleaves diacylglyceryl-prolipoprotein at the amino-terminal end of diacylated cysteine⁺¹, resulting in apolipoprotein and a signal peptide. The latter is degraded by the action of SppA, also known as factor IV (23, 25). The third step is catalyzed by apolipoprotein *N*-acyltransferase (Lnt) that adds a palmitate (C_{16:0}), derived from *sn*-1 of phosphatidylethanolamine, to the free α -amino group of cysteine⁺¹, resulting in triacylated lipoproteins (21). This reaction proceeds via the formation of a thioester acyl-enzyme intermediate in which the active-site cysteine becomes acylated (6, 60). The enzymes Lgt and Lsp are conserved in all classes of bacteria,

whereas Lnt is only present in *Proteobacteria*, *Actinobacteria*, and *Spirochetes* (56, 60, 63). Recent reports, however, demonstrated that triacylated lipoproteins exist at least in the *Staphylococcus* species of Gram-positive bacteria (32) and in *Mollicutes* (50). This suggests that they might also possess *N*-acyltransferase activity.

Biochemical studies on Lgt demonstrated that it is membrane bound (54) and that it can be solubilized in an active form in *N*-octyl- β -D-glucoside (48). The gene encoding *lgt* was first identified by Gan et al. (15) through characterization of a temperature-sensitive mutant of *Salmonella enterica* serovar Typhimurium that accumulates unmodified Lpp at a restrictive temperature (15). The gene is allelic to the gene encoding unidentified membrane protein A (*umpA*) of *Escherichia coli* (64). An *lgt*(Ts) mutant of *E. coli* can be complemented by *lgt* from *Staphylococcus aureus*, illustrating that Lgt proteins of different species are functionally conserved (43). Recent studies demonstrated that deletion of *lgt* attenuates virulence in Gram-positive bacteria (5, 20, 39), while others report that the contribution of Lgt is limited or that its absence enhances virulence (18, 35, 63).

The functional characterization of Lgt is key to understanding the mechanism by which lipoproteins function as virulence factors and to developing methods that will contribute to finding new antibacterial agents. To gain insight into how Lgt recognizes and/or binds its substrates, phosphatidylglycerol and prolipoprotein, its membrane topology was determined and essential residues were identified.

Received 5 December 2011 Accepted 19 January 2012

Published ahead of print 27 January 2012

Address correspondence to Nienke Buddelmeijer, niebud@pasteur.fr.

Supplemental material for this article may be found at <http://jb.asm.org/>.

Copyright © 2012, American Society for Microbiology. All Rights Reserved.

doi:10.1128/JB.06641-11

(<http://bioinf.cs.ucl.ac.uk/psipred>), PHDHTM (http://npsa-pbil.ibcp.fr/cgi-bin/npsa_automat.pl?page=/NPSA/npsa_htm.html), SOSUI (http://bp.nuap.nagoya-u.ac.jp/sosui/sosui_submit.html), PHOBIUS (<http://phobius.sbc.su.se>), OCTOPUS (<http://phobius.sbc.su.se>), TOPPED (<http://www.sbc.su.se/~erikw/topped2>), and TMHMM (<http://www.cbs.dtu.dk/services/TMHMM>).

A BLASTP search (<http://blast.ncbi.nlm.nih.gov>) using the sequence with accession number NP_417305 was performed on bacterial genomes to identify conserved residues in Lgt. A total of 1,542 sequences (with an E-value of <0.01) were obtained, and sequences annotated as Lgt (446 sequences) were further analyzed. A sequence alignment was made using CLUSTALW (<http://www.ebi.ac.uk/Tools/msa/clustalw2>). To facilitate the analysis, sequences from Gram-negative bacteria and Gram-positive bacteria were aligned separately. Species-specific residues were identified, as well as common conserved amino acids.

Cell fractionation and separation of inner membrane and outer membrane by sucrose flotation gradient. Cells from a 100-milliliter culture were broken by two passages through a French pressure cell at 10,000 lb/in². The membrane and soluble fractions were separated as described previously (44). The inner and outer membranes were separated by sucrose flotation gradient centrifugation (44). Twenty-one fractions of 250 μ l were collected, and 10 μ l of each was loaded on SDS-PAGE.

Lgt solubilization from membrane vesicles. Membrane vesicles prepared as described above were resuspended in 0.75 M NaCl, 8 M urea, 4 M urea, or 1% *N*-octyl- β -D-glucoside (β -OG) in TED buffer (20 mM Tris-HCl, pH 8.0, 1.25 mM EDTA, 2 mM dithiothreitol [DTT]). Samples were incubated for 1 h at 4°C. The membrane and soluble fractions were separated by ultracentrifugation for 30 min at 135,000 \times g and analyzed by SDS-PAGE and immunoblotting.

SCAM. For the substituted cysteine accessibility method (SCAM) analysis, two 1-ml amounts of cells of an OD₆₀₀ of 1 were centrifuged for 3 min at 16,000 \times g. Cells were washed twice in phosphate buffer (PB) (50 mM KP_i, pH 7.0). Each pellet was resuspended in 120 μ l of PB, EDTA was added to a final concentration of 2.5 mM, and the cell suspension was gently mixed. The membrane-impermeable reagent (2-sulfonatoethyl)-methane thiosulfonate (MTSES) was added to a final concentration of 30 mM to one tube, and the equivalent volume of water was added to the second tube. After incubation for 30 min at 4°C, 100 mM L-cysteine was added to quench the reaction. Cells were kept at 4°C for 15 min and washed three times in PB. Pellets were resuspended in 50 μ l PB, and proteins were precipitated in 10% trichloroacetic acid (TCA) for 1 h on ice. Samples were conserved at -20°C overnight. Protein pellets were collected by centrifugation at 16,000 \times g for 20 min at 4°C and washed twice with acetone. Pellets were air dried and resuspended in 100 μ l PEG buffer (1 M Tris-HCl, pH 7.0, 10 M urea, 1% SDS, and 1 mM EDTA) and incubated for 30 min at room temperature. Polyethylene glycol 5000-maleimide (MalPEG) was added to a final concentration of 0.24 mM to all samples that were incubated at room temperature for 1 h. After dilution in 10 volumes of water, proteins were TCA precipitated for 3 h on ice, collected, and washed as described above. Pellets were air dried overnight and resuspended in SDS sample buffer.

Live-cell imaging. PAP9403 and PAP9405 were grown in the presence or absence of 0.2% L-arabinose. At different time intervals, 1 ml of cell culture was harvested and centrifuged. Pellets were resuspended in fresh LB. Cell membranes were stained with a final concentration of 3 μ g ml⁻¹ FM-1-43 and the DNA with a final concentration of 1 μ g ml⁻¹ Hoechst stain number 33342. Cells were stained for 30 min at room temperature and washed once in LB. Cells were immobilized on a thin layer of 1% agarose in water and visualized by phase-contrast and epifluorescence microscopy using a Zeiss AxioScope-2 microscope coupled with a Zeiss charge-coupled device (CCD) camera. Membrane fluorescence (green) was detected with a filter for green fluorescent protein (GFP) and DNA fluorescence (blue) with a filter for 4',6'-diamidino-2-phenylindole (DAPI). Images were acquired using AxioVision (Zeiss) and processed with Photoshop.

Complementation assay. Cysteine and alanine mutants of *Lgt* cloned into a pAM238 vector were transformed into PAP9403. Transformants were selected on plates containing spectinomycin and chloramphenicol in the presence of L-arabinose. After incubation at 37°C overnight, isolated colonies were restreaked on plates containing or not containing L-arabinose and supplemented or not supplemented with IPTG. Plates were kept at 37°C overnight, and the ability to restore growth was analyzed for each Lgt variant.

SDS-PAGE and immunoblotting. Protein samples were resuspended in SDS sample buffer containing 100 mM DTT and heated at 100°C for 5 min. Samples were separated on a 10% polyacrylamide gel (SDS-PAGE), and proteins were transferred onto nitrocellulose membranes. Different forms of Lpp were analyzed on 18% Tris-tricine SDS-PAGE, followed by immunodetection. Membranes were incubated with primary antibody against c-myc (Sigma) or mCherry (Chemicon) to detect Lgt fusion proteins or with polyclonal antisera against OmpA (provided by U. Henning), DjlA (provided by D. Clarke), or Lpp (provided by H. Tokuda). Secondary antibodies against mouse or rabbit immunoglobulins conjugated with horseradish peroxidase were detected by chemiluminescence (Pierce).

RESULTS

In silico membrane topology prediction of Lgt of *E. coli*. Eight different topology prediction algorithms were used to determine the membrane topology of Lgt; HMMTOP (57), MEMSAT (26), PHDHTM (45), SOSUI (22), PHOBIUS (27), OCTOPUS (61), TOPPED (9), and TMHMM (30) (see Materials and Methods). The programs are based on different methods, which improves the reliability of the prediction (38). The majority of the algorithms predicted seven transmembrane segments (TMS), whereas TMHMM predicted five TMS (Fig. 2). Both models are in agreement with previous results that demonstrated that the C terminus of Lgt faces the cytoplasm (10).

Lgt is an integral inner membrane protein. *In silico* analysis of Lgt suggests that it is an integral multispreading membrane protein. The membrane localization of Lgt was determined by detergent solubilization and by separation of membranes by sucrose flotation gradients. Antibodies raised against a synthetic peptide (F₁₁₆ARRTKRSFFQVSD₁₂₉C) did not allow the detection of chromosomal or plasmid-encoded Lgt by immunoblotting. Therefore, two Lgt fusion proteins were created, Lgt with a C-terminal double c-myc tag (Lgt-c-myc₂ encoded by pCHAP9224; c-myc₂ is composed of 20 amino acids) or fused to mCherry (Lgt-mCherry encoded by pCHAP9296; mCherry is composed of 237 amino acids) (Table 1). High salt (0.75 M) did not release Lgt-c-myc₂ or Lgt-mCherry from membrane preparations, and 8 M urea only partially released the Lgt fusion proteins (Fig. 3A and C). These data show that Lgt-c-myc₂ and Lgt-mCherry are not peripherally associated with the inner membrane. The nonionic detergent *N*-octyl- β -D-glucoside completely solubilized both Lgt fusion proteins from membrane vesicles, illustrating that they are membrane embedded (Fig. 3A and C).

To determine whether the Lgt fusion proteins are located in the inner membrane, the inner and outer membranes were separated on a sucrose flotation gradient. Lgt-c-myc₂ and Lgt-mCherry were observed in less dense fractions corresponding to the inner membrane, together with DjlA that was used as an inner membrane reference protein, and distinct from outer membrane fractions containing OmpA (Fig. 3B and D). Both Lgt-c-myc₂ and Lgt-mCherry complemented an *Lgt* depletion strain (see below), indicating that they are functional.

Lgt has seven transmembrane segments. A classical gene fu-

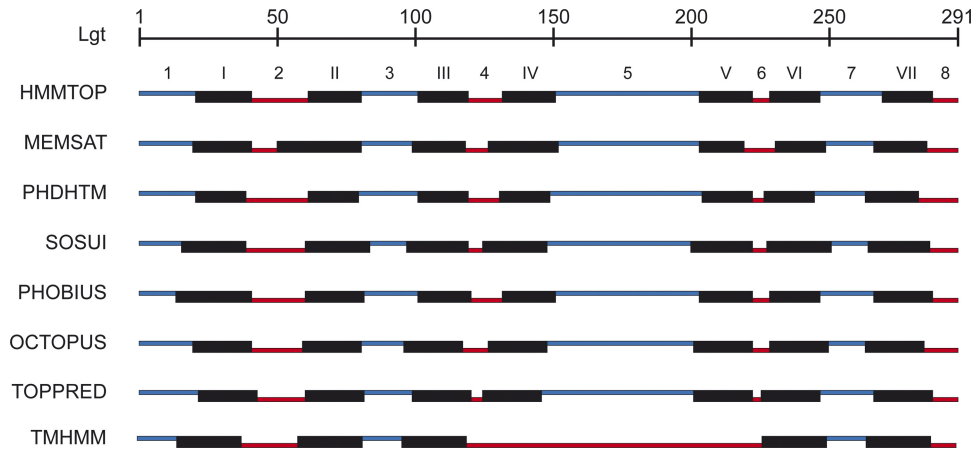


FIG 2 Membrane topology predictions for Lgt of *E. coli*. Eight different algorithms were used to predict the membrane topology of Lgt of *E. coli*. Lgt is composed of 291 amino acids, indicated at top. Black boxes (I to VII) represent transmembrane segments (TMS), blue lines (1, 3, 5, and 7), correspond to periplasmic loops, and red lines (2, 4, 6, and 8) correspond to cytoplasmic loops.

sion approach using *lacZ* (encoding β -galactosidase) and *phoA* (encoding alkaline phosphatase) was used to determine the membrane topology of Lgt (36, 55). Alkaline phosphatase is only active when it is translocated through the cytoplasmic membrane into the periplasm, and it is inactive when localized to the cytoplasm. In contrast, β -galactosidase is active when localized in the cytoplasm. Fusion of PhoA to a periplasmic site of a membrane protein yields a hybrid protein with the PhoA moiety in the periplasm and thus with alkaline phosphatase activity. Similarly, hybrid proteins with LacZ fusions to cytoplasmic stretches of a membrane protein yield β -galactosidase activity. The membrane topology of Lnt was determined previously using LacZ and PhoA fusion proteins (44). Full-length Lnt (Lnt⁵¹²) has high β -galactosidase activity when fused to LacZ and low alkaline phosphatase activity when

fused to PhoA; therefore, the C terminus is located in the cytoplasm. Lnt⁴⁷⁶ has high alkaline phosphatase activity and low β -galactosidase activity, positioning this residue in the periplasm. These hybrid proteins were used here as controls.

Lgt fragments of various lengths were amplified by PCR and cloned into plasmids pCHAP6577 and pCHAP6578, resulting in *lacZ* and *phoA* fusions, respectively (44). Each potential cytoplasmic and periplasmic loop was fused to LacZ and PhoA, except for the first N-terminal periplasmic domain (Fig. 2). Immunoblotting using anti-LacZ antibodies revealed that all Lgt-LacZ fusion proteins were produced, although some processing was observed for LacZ hybrid proteins fused to A163, P221, and A250. Hybrid proteins with junction sites after G51, A163, and S291 showed relatively high LacZ and low PhoA activities (Fig. 4A and B). This

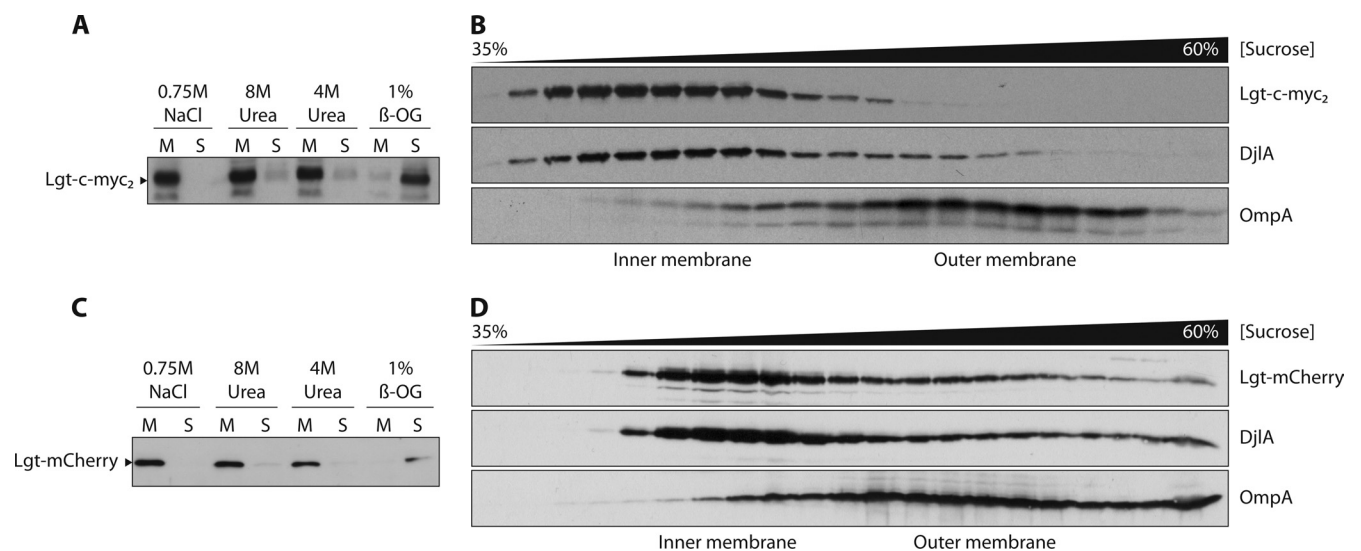


FIG 3 Lgt-c-myc₂ and Lgt-mCherry are polytopic inner-membrane proteins. Membrane vesicles of *E. coli* containing either Lgt-c-myc₂ (encoded by pCHAP9224) or Lgt-mCherry (encoded by pCHAP9296) were isolated and treated with 0.75 M NaCl, 8 M urea, 4 M urea, or 1% *N*-octyl- β -D-glucoside (β -OG). Soluble (S) and membrane (M) fractions were analyzed by SDS-PAGE and immunoblotting using anti-c-Myc (A) or anti-mCherry (C) antibodies. Inner and outer membranes were separated by flotation sucrose gradients. The presence of Lgt-myc₂ (B) and Lgt-mCherry (D) was analyzed in each of the fractions by SDS-PAGE and immunoblotting. Anti-DjlA and anti-OmpA antibodies were used to identify fractions corresponding to the inner and the outer membrane, respectively.

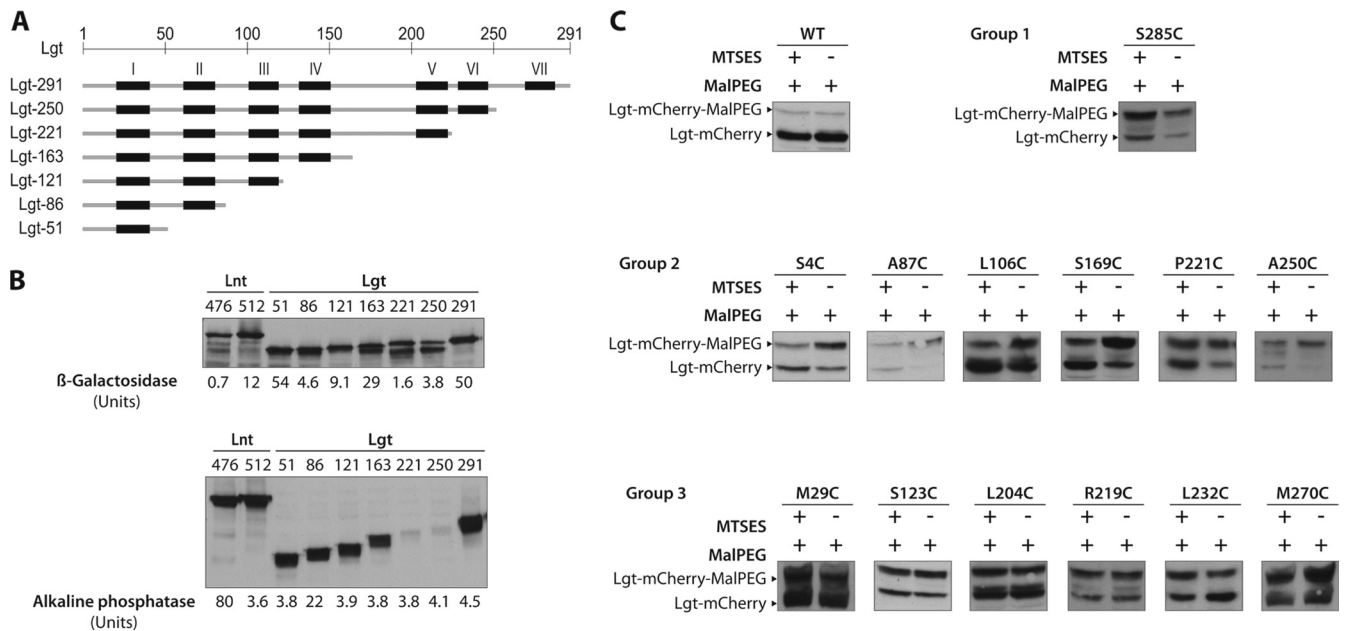


FIG 4 SCAM analysis of Lgt^{Cys}-mCherry mutants. (A and B) Production and enzyme activities of Lgt-β-galactosidase and Lgt-alkaline phosphatase fusion proteins. Lnt fusion proteins were included as controls (44). (C) *E. coli* cells overproducing functional single cysteine variants of Lgt-mCherry were treated (+) or not (-) with MTSES. After precipitation and denaturation, proteins were alkylated by MalPEG. Proteins were separated on SDS-PAGE, and Lgt-mCherry was detected by immunoblotting using anti-mCherry antibodies. Bands corresponding to alkylated (Lgt-mCherry-MalPEG) and nonalkylated Lgt (Lgt-mCherry) are indicated. WT, wild type.

suggests that residues G51, A163, and S291 are located in the cytoplasm. The cytoplasmic location of residue S291 is in agreement with previous findings (10). No LacZ activity was observed with hybrids with junction sites after M86, K121, P221, and A250. All Lgt-PhoA fusion proteins were detectable by immunoblotting, but hybrid proteins created at junctions P221 and A250 in Lgt were less abundant (Fig. 4A and B). Alkaline phosphatase activity was detected only with M86; since this hybrid protein did not show any LacZ activity, this result suggests that M86 is located in the periplasm. Enzymatic activity could not be measured with PhoA hybrids with junction sites after G51, K121, A163, P221, A250, and S291 in Lgt. In the cases of Lgt^{P221}-PhoA and Lgt^{A250}-PhoA, this might have been due to low protein levels, but all other PhoA hybrid proteins were as abundant as Lgt^{M86}-PhoA. The hybrid proteins with junctions close to the membrane interface, such as K121 and P221, seemed to have altered folding of LacZ, resulting in inactive enzymes. Taken together, the results indicate that Lgt is embedded in the inner membrane via at least three transmembrane segments, TMS I, TMS II, and TMS III, and that its C terminus is located in the cytoplasm.

A second approach, the substituted cysteine accessibility method (SCAM), was used to determine the topology of Lgt more precisely (4). SCAM is based on the accessibility of cysteine residues to thiol-specific reagents and involves two steps. In the first step, cells were treated with the membrane-impermeable reagent (2-sulfonatoethyl)-methane thiosulfonate (MTSES). MTSES reacts with free thiol groups of cysteine residues facing the periplasm but not of those located in the cytoplasm or membrane. In the second step, precipitated proteins were treated with polyethylene glycol 5000-maleimide (MalPEG), resulting in alkylation of (free) thiol groups that did not previously react with MTSES. Thus, MalPEG reacts with cysteines located in the cytoplasm. The entire Lgt

protein was analyzed, rather than truncated fragments as used in the LacZ and PhoA topology mapping. Lgt does not contain cysteine residues.

Sixteen single cysteine variants (Lgt^{Cys}) were constructed by replacement of nonconserved amino acids such that each potential extramembrane loop contained one cysteine residue. Cysteine substitutions were also made in residues in predicted transmembrane segments. The production of several Lgt^{Cys} variants was slightly lower than the production of wild-type Lgt, both as c-myc₂ and mCherry fusion proteins (see Fig. S1 in the supplemental material). In two cases, Lgt^{R219C}-mCherry and Lgt^{S285C}-mCherry resulted in higher levels of protein production than the corresponding c-myc₂ fusion proteins (see Fig. S1). All Lgt^{Cys} variants except Lgt^{S50C}, Lgt^{L134C}, and Lgt^{A163C} were functional, as shown by complementation of an *lgt* depletion strain (see below).

Only functional Lgt^{Cys}-mCherry proteins were used for the SCAM analysis, which allowed the identification of three groups of cysteine replacements (Fig. 4C). The cysteine in Lgt^{S285C}-mCherry was alkylated by MalPEG to the same extent irrespective of MTSES treatment, suggesting that S285C is not accessible to MTSES and consistent with its cytoplasmic location. Cysteines in Lgt^{S4C}-mCherry, Lgt^{A87C}-mCherry, Lgt^{L106C}-mCherry, Lgt^{S169C}-mCherry, Lgt^{P221C}-mCherry, and Lgt^{A250C}-mCherry were accessible to MTSES, resulting in less alkylated protein than in samples not treated with MTSES before the MalPEG treatment. These results suggest that S4, A87, L106, S169, P221, and A250 are facing the periplasm. Cysteines in Lgt^{M29C}-mCherry, Lgt^{S123C}-mCherry, Lgt^{L204C}-mCherry, Lgt^{R219C}-mCherry, Lgt^{L232C}-mCherry, and Lgt^{M270C}-mCherry demonstrated poor accessibility to MTSES, since the degree of alkylation by MalPEG was not affected by MTSES, but alkylation was less efficient than with Lgt^{S285C}-



FIG 5 Depletion of *lgt* leads to accumulation of Pro-Lpp. Lpp was detected by Western blotting of total cell lysates of PAP9403 grown in the presence (+) and absence (-) of L-arabinose with anti-Lpp antibodies. Samples were taken after 180 min according to the results of the growth experiment shown in Fig. 6A. a, mature (triacylated) Lpp; b, pro-Lpp; *, degradation product derived from pro-Lpp; Δ, a form of pro-Lpp most likely linked to peptidoglycan fragments.

mCherry. These data suggest that M29, S123, L204, R219, L232, and M270 are located in the membrane.

In both the five-TMS and the seven-TMS topology model, residues S4, A87, and A250 are located in the periplasm, residues M29 and M270 are embedded in the membrane, and S285 is located in the cytoplasm, consistent with the SCAM results. The data obtained with S169 clearly show that this residue is facing the periplasm and that L204 and L232 are embedded in the membrane, suggesting the existence of TMS V and TMS VI. S123, R219, and P221 are predicted to be cytoplasmic in both models. The SCAM results obtained with S123 are in agreement with those obtained with the LacZ and PhoA fusion proteins to Lgt^{K121}; S123 is partially embedded in the membrane. R219 is also membrane embedded, unlike P221, which is accessible to MTSES. These data are more difficult to interpret and may suggest a dynamic orientation of Lgt in the membrane; however, identical results were obtained three times with the SCAM analysis. In conclusion, Lgt is embedded in the cytoplasmic membrane via seven transmembrane segments.

Lgt is essential for growth, and the majority of essential residues are located in the membrane. To determine the effect of *lgt* depletion on lipoprotein modification and to identify essential residues in Lgt, an *lgt* depletion strain was constructed by disrupting the chromosomal *lgt* gene by allelic replacement (11). Replacement of *lgt* with a Km^r cassette with 500 base pairs homologous to the chromosomal region surrounding *lgt* at each extremity was obtained by recombination between the chromosomal locus and a 2-kb PCR product. The 10 base pairs at the 3' extremity of *lgt* were left intact because of the transcriptional coupling between *lgt* and the downstream gene *thyA* (16). Since Lgt is an essential protein (64), the mutation was constructed in a strain with a second copy of *lgt* under tightly controlled P_{ara} promoter control (pCHAP9231). The *lgt* depletion strain (PAP9403) did not form colonies on plates without L-arabinose (data not shown). Depletion of *lgt* led to the accumulation of pro-Lpp, illustrating that in the absence of Lgt, lipoproteins are no longer modified with an S-diacylglyceryl group (Fig. 5).

The growth of the *lgt* depletion strain was monitored in the presence and absence of 0.2% L-arabinose (Fig. 6A). The growth of the *lgt* depletion strain in the presence of L-arabinose was similar to that of the wild type, and a growth defect was observed after 120 min without L-arabinose. The phenotype of cells of PAP9403 was analyzed after 30, 120, and 275 min of growth in the presence or absence of L-arabinose (Fig. 6B). PAP9403 grown without L-arabinose exhibited an atypical shape, with one pointed pole from which DNA leakage could occasionally be observed. After 275 min, a mixture of lysed and enlarged cells was observed. These cells were stained with FM 1-43 but not with Hoechst stain num-

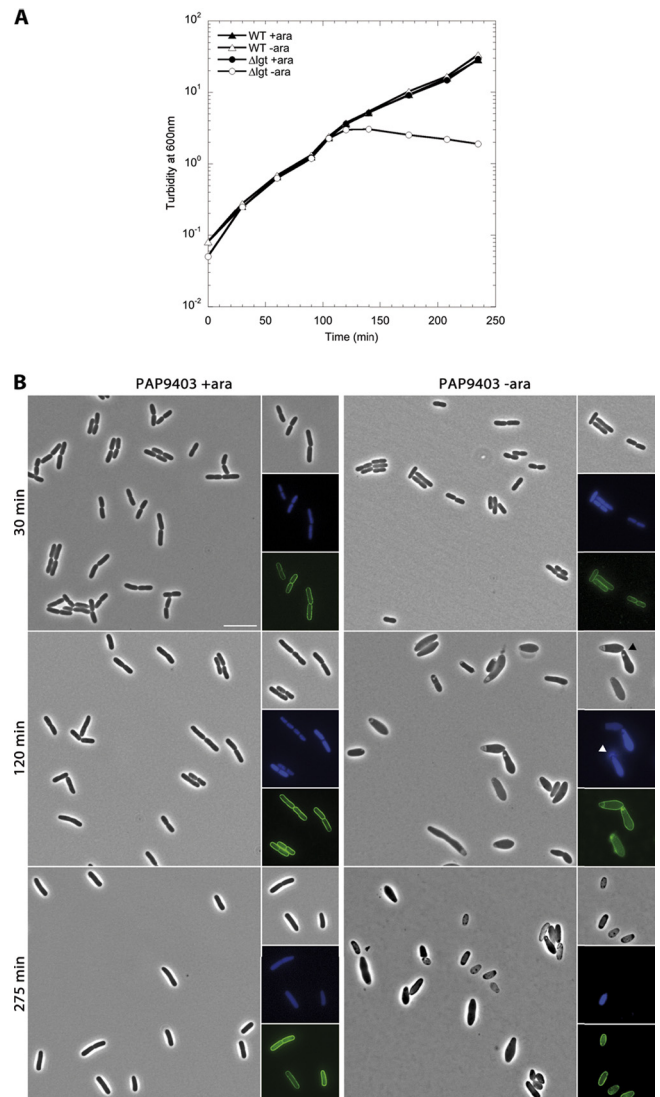


FIG 6 Growth curve and phenotype of the *lgt* depletion strain. (A) Reproducible and representative growth curve of PAP9403 grown in LB in the presence (+ara) or absence (-ara) of 0.2% L-arabinose. PAP9405 was used as the wild-type (WT) strain. The cultures were kept in exponential phase by serial dilutions. (B) The phenotype of PAP9403 was observed in separate experiments from those whose results are shown in panel A. Nucleoids were stained with Hoechst stain number 33342 (blue), and the outer membrane with FM-1-43 (green). Cells were observed by phase-contrast (large and upper small panels) and fluorescence microscopy (center and bottom small panels). White arrowhead indicates DNA leakage. Bar represents 2 μ m.

ber 33342, suggesting the presence of intact outer membranes but a lack of DNA due to leakage. This morphology is similar to that observed for SE5221 [*lgt*^{D249N}(Ts)] of *S. enterica* serovar Typhimurium grown under restrictive conditions (15).

The *E. coli* Lgt sequence was used as a query in a BLASTP search to identify Lgt in all bacterial genomes available at the time of the study. Of a total of 1,542 sequences, 446 sequences annotated as Lgt (based on the Lgt signature motif), including 96 in *Firmicutes*, 32 in *Actinobacteria*, and 318 in *Proteobacteria*, were analyzed further. Sequences derived from each group of bacteria were first aligned separately and then compared. Residues Y26, G99, G104, R143, and G154 are highly conserved in all bacteria. D129 is con-

TABLE 2 Complementation of an *lgt* depletion strain by Lgt^{Ala}-*c-myc*₂ variants

Mutation	Complementation ^a	Location ^b
Y26A	–	TMS I
G98A	+	TMS III
G104A	+	TMS III
D129A	+	TMS IV
R143A ^c	+/-	TMS IV
N146A ^c	–	TMS IV
E151A ^c	+/- ^d	Loop 5
G154A ^c	–	Loop 5
R239A	+/-	TMS VI
E243A	+/-	TMS VI
H103Q ^e	+	TMS III

^a +, full complementation; +/-, partial complementation; –, no complementation of PAP9403 on plates without L-arabinose containing 1 mM IPTG.

^b Location as shown in Fig. 2.

^c Residue is in Lgt signature.

^d Colony morphology was mixed.

^e Mutation was previously identified (46).

served in *Firmicutes* and in *Proteobacteria*, with the exception of *Francisella* strains, which have E at this position. G71, N146, E151, and R239 are conserved in *Actinobacteria* and *Proteobacteria*, and E243 is only totally conserved in *Proteobacteria*. G33, R73, G98, P133, G142, G145, and L200 are conserved in *Actinobacteria*. We did not identify any residues that are conserved only in *Firmicutes* or in *Firmicutes* and either *Actinobacteria* or *Proteobacteria* (see Table S2 in the supplemental material).

These highly conserved amino acids in *E. coli* Lgt (Y26, G104, D129, R134, N146, E151, G154, R239, and E243) were replaced with alanine by site-directed mutagenesis, with the exception of G71 and G99 but including G98, and the effect on Lgt function was tested *in vivo* in a complementation assay using the *lgt* depletion strain. The H103Q mutation, which was previously shown to result in inactive enzyme, was also included in the analysis (46). H103 is not conserved in the different bacteria (see Table S2). The *lgt*^{Ala}-*c-myc*₂ genes were expressed from a P_{lac} promoter (pAM238-derived plasmid) in the *lgt* depletion strain grown in the absence of L-arabinose with or without IPTG. Under these conditions, the expression of *lgt* from P_{ara} on pCHAP9231 is repressed and *lgt* variants are expressed from P_{lac} by induction with IPTG. Lgt^{Y26A}, Lgt^{N146A}, and Lgt^{G154A} do not restore the growth of the *lgt* depletion strain even in the presence of IPTG, indicating that these residues are required for Lgt function (Table 2). Lgt^{R143A}, Lgt^{E151A}, Lgt^{R239A}, and Lgt^{E243A} all partially restored the growth of the *lgt* depletion strain, meaning that few colonies were formed after growth on plates lacking L-arabinose. Lgt^{G98A}, Lgt^{G104A}, Lgt^{D129A}, and Lgt^{H103Q} are not essential, since the growth of the *lgt* depletion strain was fully restored in the absence of L-arabinose. All Lgt variants were produced and the addition of IPTG slightly in-

creased the protein levels, although the protein levels varied depending on the substitution (Fig. 7). The nonfunctional protein Lgt^{Y26A} was highly overproduced compared to the production of wild-type Lgt but did not have a dominant negative effect in a wild-type background (data not shown). Lgt^{N146A} and Lgt^{G154A} were also less abundant than the wild type, and a C-terminal degradation product was detected (data not shown). The addition of IPTG did not increase the protein levels of Lgt^{G154A}. In this case, the protein levels may not be sufficient to observe complementation of the *lgt* depletion strain. The protein levels of functional Lgt^{G98A} and Lgt^{G104A} and partially functional Lgt^{E151A} were comparable to the levels of Lgt^{Y26A}. Lgt^{D129A}, Lgt^{R143A}, Lgt^{R239A}, and Lgt^{E243A} were less abundant than wild-type Lgt. These data illustrate that low levels of Lgt are sufficient to complement the *lgt* depletion strain and that protein levels and functionality are not directly correlated.

DISCUSSION

E. coli Lgt is an integral inner membrane protein with seven transmembrane segments. Previous work by Selvan and Sankaran suggested that Lgt is not membrane embedded and that it is in fact a water-soluble protein (49). Overexpression of *lgt* from a strong promoter on a high-copy-number plasmid probably resulted in small, membrane-associated aggregates in the reported study. Lgt activity in the water-soluble fraction without detergent observed by Selvan and Sankaran is difficult to explain in light of the data presented here. Furthermore, Lgt is only active in certain detergents (47, 54).

The membrane topology of the other two lipoprotein-modifying enzymes, Lsp and Lnt, was more straightforward to determine than that of Lgt. Analysis of LacZ and PhoA fusion proteins showed that Lsp spans the membrane four times (37) and that Lnt has six transmembrane segments (44). Similar fusion proteins with Lgt confirmed the cytoplasmic localization of its C terminus and validated predicted TMS I, II, and III. The SCAM analysis provided evidence that Lgt has seven and not five TMS (summarized in Fig. 8).

The phenotype of the *lgt* depletion strain, with cell lysis occurring at one pole, is intriguing. Cell division filaments of *E. coli* treated with cefsulodin, which preferentially bind to PBP1a and -1b, lyse at potential cell division sites where new peptidoglycan is synthesized (12). Recent reports have identified two outer-membrane lipoproteins, LpoA and -B, involved in PBP1a and -1b activity, respectively (41, 58). We hypothesize that under *lgt* depletion conditions, LpoA and -B do not possess an S-diacylglyceryl modification and are therefore mislocalized to the inner membrane, leading to deficient peptidoglycan synthesis. This indirectly suggests that lysis of the *lgt* depletion mutant occurs at the new pole.

Essential residues were identified previously in a complementation assay using the *lgt*(Ts) (Lgt^{G104S}) mutant SK634 of *E. coli*

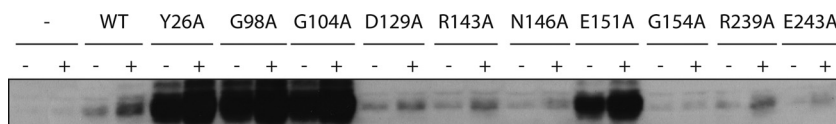


FIG 7 Protein production of Lgt^{Ala} variants. Comparison of protein levels of 10 Lgt^{Ala}-*c-myc*₂ variants. The proteins were produced in PAP105 in the absence (–) or presence (+) of 1 mM IPTG. The proteins were analyzed by immunoblotting with anti-*c-myc* antibodies. All fractions loaded were derived from the same volume of bacterial suspension. WT, wild type.

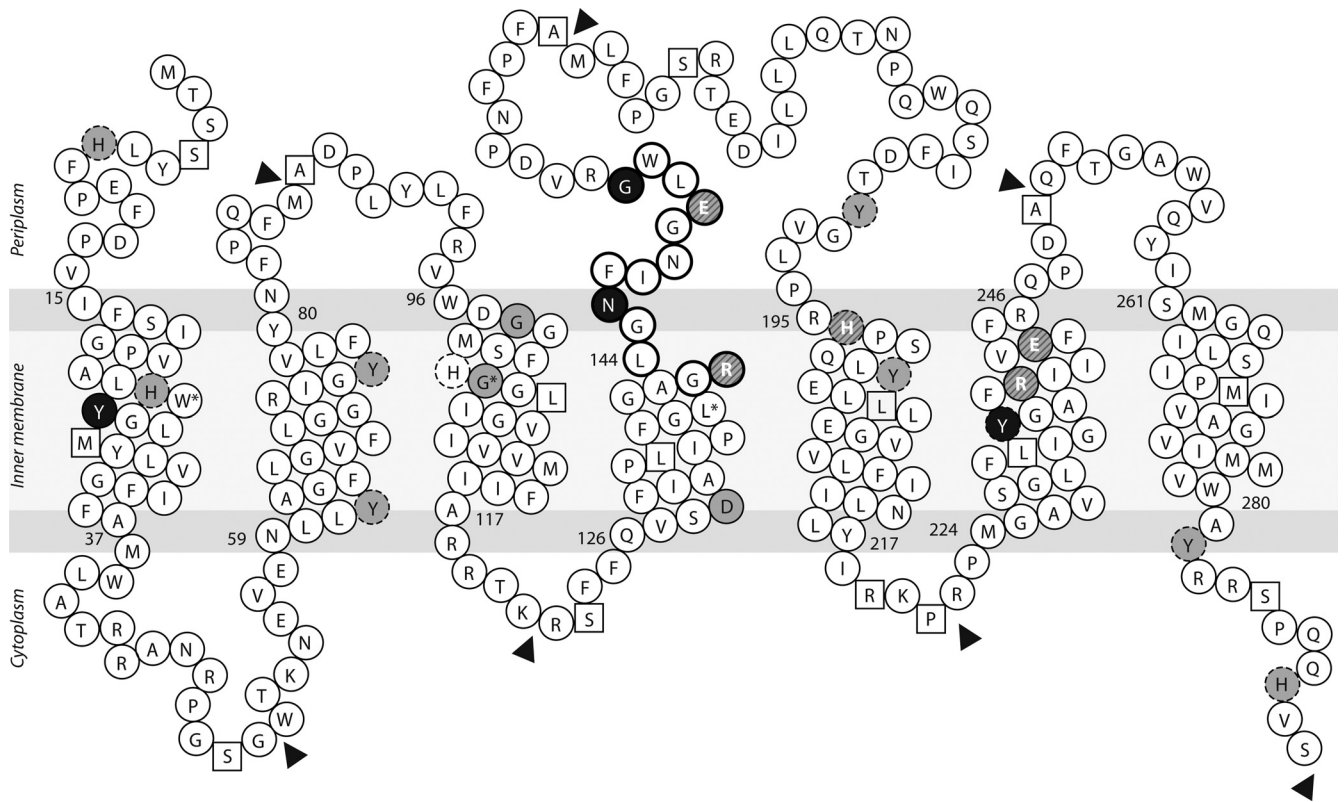


FIG 8 Lgt membrane topology and essential residues. Lgt is anchored in the inner membrane by seven TMS, and the C terminus faces the cytoplasm. Residues of the Lgt signature are circled in bold. Arrowheads indicate β -galactosidase and PhoA fusion proteins with Lgt. Black filled circles indicate essential residues, gray circles nonessential residues, and hatched circles important residues. Residues identified previously are shown by dotted circles (see text for details). Residues replaced with cysteines for the SCAM analysis are illustrated as squares. Asterisks refer to *lgt*(Ts) mutants, W25, G104, and L139.

and by kinetic analysis using a synthetic peptide (46). Although the total amount of membrane protein in the assay was identical for each Lgt variant, the protein levels of Lgt enzymes were not determined. The H103Q/N substitutions resulted in nonfunctional proteins. In our hands, however, H103Q is functional *in vivo*. The Y26A substitution described here also rendered Lgt inactive; however, Y26F was functional (46). The Y235T/F substitutions inactivated the enzyme, and Lgt with Y235S had reduced (60%) activity. These residues are all embedded in the membrane. The H169R/Q substitutions also reduced enzymatic activity (50%), while H169N/L did not affect Lgt activity (46). Other substitutions that resulted in partially active mutants include R143A, R239A, and E243A. These residues are also located in the membrane. Two other *lgt*(Ts) strains of *E. coli* have been reported, SK636 encoding Lgt^{W25R} and SK635 encoding Lgt^{L139F}; both residues are located in the membrane (43, 64). These residues are probably involved in protein stability and/or folding rather than catalytic activity.

Two substitutions in the Lgt signature motif, N146A and G154A, also inactivated the protein. These residues are located at the membrane-periplasm interface, together with the important residue E151. A region in the N terminus of Lgt resembles an acyltransferase motif (HX₃DX₁₄Y) found in acyltransferases implicated in mycobacterial polyketide biosynthesis (2), with the only differences being that H7 and D12 are separated by four amino acids rather than three and that 13 residues instead of 14 separate D12 from Y26 (HX₄DX₁₃Y). The role of this motif in

acyltransferases is not well defined. One possibility is that it is involved in the binding or recognition of phosphatidylglycerol together with the Lgt signature motif. This glycine-rich region, including R143, is reminiscent of phosphate-binding loops (34). Y235 and H103 were suggested to play a role in catalytic activity (46). These residues, however, are not highly conserved among bacterial species. The prototypical acyltransferases PlsB and PlsC contain four conserved blocks of amino acids, among which is the HX₄D motif that is implicated in catalysis (19, 33). PlsY also contains distinct sequences, including HKDNX₈E, that are not shared with PlsB and PlsC (34). Lgt does not have motifs in common with these acyltransferases.

The present study demonstrates that the protein levels and functionality of single amino acid variants are not directly correlated. It seems that slight changes in amino acid composition either reduce protein levels, either because of lower production or instability, or increase protein levels. The data presented here suggest that the active site of Lgt is embedded in the membrane. Other examples of catalytic-site-embedded enzymes are intramembrane proteases, also known as i-CLiPs or rhomboid proteases (for reviews, see references 14 and 59). *E. coli* GlpG is a member of this family. Structural analysis showed that its active site is embedded in the membrane and water accessible from the periplasmic side of the membrane (1, 62, 65). We hypothesize that Lgt has such a putative active-site pocket. It would be very intriguing to see whether Lgt shares similar structural aspects with GlpG and how it interacts with its substrates.

ACKNOWLEDGMENTS

We are grateful to all members of the Molecular Genetics Unit for their helpful comments and suggestions. We thank Nicolas Bayan and Tony Pugsley for critical reading of the manuscript.

REFERENCES

- Ben-Shem A, Fass D, Bibi E. 2007. Structural basis for intramembrane proteolysis by rhomboid serine proteases. *Proc. Natl. Acad. Sci. U. S. A.* 104:462–466.
- Bhatt K, Gurcha SS, Bhatt A, Besra GS, Jacobs WR, Jr. 2007. Two polyketide-synthase-associated acyltransferases are required for sulfolipid biosynthesis in *Mycobacterium tuberculosis*. *Microbiology* 153:513–520.
- Binet R, Wandersman C. 1995. Protein secretion by hybrid bacterial ABC-transporters: specific functions of the membrane ATPase and the membrane fusion protein. *EMBO J.* 14:2298–2306.
- Bogdanov M, Zhang W, Xie J, Dowhan W. 2005. Transmembrane protein topology mapping by the substituted cysteine accessibility method (SCAM(TM)): application to lipid-specific membrane protein topogenesis. *Methods* 36:148–171.
- Bubeck Wardenburg J, Williams WA, Missiakas D. 2006. Host defenses against *Staphylococcus aureus* infection require recognition of bacterial lipoproteins. *Proc. Natl. Acad. Sci. U. S. A.* 103:13831–13836.
- Buddelmeijer N, Young R. 2010. The essential *Escherichia coli* apolipoprotein N-acyltransferase (Lnt) exists as an extracytoplasmic thioester acyl-enzyme intermediate. *Biochemistry* 49:341–346.
- Cascales E, Bernadac A, Gavioli M, Lazzaroni JC, Lloubes R. 2002. Pal lipoprotein of *Escherichia coli* plays a major role in outer membrane integrity. *J. Bacteriol.* 184:754–759.
- Choi D-S, Yamada H, Mizuno T, Mizushima S. 1986. Trimeric structure and localization of the major lipoprotein in the cell surface of *Escherichia coli*. *J. Biol. Chem.* 261:8953–8957.
- Claros MG, von Heijne G. 1994. TopPred II: an improved software for membrane protein structure predictions. *Comput. Appl. Biosci.* 10:685–686.
- Daley DO, et al. 2005. Global topology analysis of the *Escherichia coli* inner membrane proteome. *Science* 308:1321–1323.
- Datsenko KA, Wanner BL. 2000. One-step inactivation of chromosomal genes in *Escherichia coli* K-12 using PCR products. *Proc. Natl. Acad. Sci. U. S. A.* 97:6640–6645.
- de Pedro MA, Høltje JV, Schwarz H. 2002. Fast lysis of *Escherichia coli* filament cells requires differentiation of potential division sites. *Microbiology* 148:79–86.
- Derbise A, Lesic B, Dacheux D, Ghigo JM, Carniel E. 2003. A rapid and simple method for inactivating chromosomal genes in *Yersinia*. *FEMS Immunol. Med. Microbiol.* 38:113–116.
- Erez E, Fass D, Bibi E. 2009. How intramembrane proteases bury hydrolytic reactions in the membrane. *Nature* 459:371–378.
- Gan K, Gupta SD, Sankaran K, Schmid MB, Wu HC. 1993. Isolation and characterization of a temperature-sensitive mutant of *Salmonella typhimurium* defective in prolipoprotein modification. *J. Biol. Chem.* 268:16544–16550.
- Gan K, et al. 1995. The *umpA* gene of *Escherichia coli* encodes phosphatidylglycerol: prolipoprotein diacylglycerol transferase (*lgt*) and regulates thymidylate synthase levels through translational coupling. *J. Bacteriol.* 177:1879–1882.
- Guzman LM, Belin D, Carson MJ, Beckwith J. 1995. Tight regulation, modulation, and high-level expression by vectors containing the arabinose PBAD promoter. *J. Bacteriol.* 177:4121–4130.
- Hamilton A, et al. 2006. Mutation of the maturase lipoprotein attenuates the virulence of *Streptococcus equi* to a greater extent than does loss of general lipoprotein lipidation. *Infect. Immun.* 74:6907–6919.
- Heath RJ, Rock CO. 1998. A conserved histidine is essential for glycerolipid acyltransferase catalysis. *J. Bacteriol.* 180:1425–1430.
- Henneke P, et al. 2008. Lipoproteins are critical TLR2 activating toxins in group B streptococcal sepsis. *J. Immunol.* 180:6149–6158.
- Hillmann F, Argentini M, Buddelmeijer N. 2011. Kinetics and phospholipid specificity of apolipoprotein N-acyltransferase. *J. Biol. Chem.* 286:27936–27946.
- Hirokawa T, Boon-Chieng S, Mitaku S. 1998. SOSUI: classification and secondary structure prediction system for membrane proteins. *Bioinformatics* 14:378–379.
- Hussain M, Ozawa Y, Ichihara S, Mizushima S. 1982. Signal peptide digestion in *Escherichia coli*. Effect of protease inhibitors on hydrolysis of the cleaved signal peptide of the major outer-membrane lipoprotein. *Eur. J. Biochem.* 129:233–239.
- Hyryläinen HL, et al. 2010. Penicillin-binding protein folding is dependent on the PrsA peptidyl-prolyl cis-trans isomerase in *Bacillus subtilis*. *Mol. Microbiol.* 77:108–127.
- Ichihara S, Beppu N, Mizushima S. 1984. Protease IV, a cytoplasmic membrane protein of *Escherichia coli*, has signal peptide peptidase activity. *J. Biol. Chem.* 259:9853–9857.
- Jones DT. 2007. Improving the accuracy of transmembrane protein topology prediction using evolutionary information. *Bioinformatics* 23:538–544.
- Kall L, Krogh A, Sonnhammer EL. 2004. A combined transmembrane topology and signal peptide prediction method. *J. Mol. Biol.* 338:1027–1036.
- Kornacki JA, Oliver DB. 1998. Lyme disease-causing *Borrelia* species encode multiple lipoproteins homologous to peptide-binding proteins of ABC-type transporters. *Infect. Immun.* 66:4115–4122.
- Kovacs-Simon A, Titball RW, Michell SL. 2011. Lipoproteins of bacterial pathogens. *Infect. Immun.* 79:548–561.
- Krogh A, Larsson B, von Heijne G, Sonnhammer E. 2001. Predicting transmembrane protein topology with a hidden Markov model: application to complete genomes. *J. Mol. Biol.* 305:567–580.
- Kumru OS, Schulze RJ, Rodnin MV, Ladokhin AS, Zuckert WR. 2011. Surface localization determinants of *Borrelia* OspC/Vsp family lipoproteins. *J. Bacteriol.* 193:2814–2825.
- Kurokawa K, Lee H, Roh et al. 2009. The triacylated ATP binding cluster transporter substrate-binding lipoprotein of *Staphylococcus aureus* functions as a native ligand for Toll-like receptor 2. *J. Biol. Chem.* 284:8406–8411.
- Lewin TM, Wang P, Coleman RA. 1999. Analysis of amino acid motifs diagnostic for the sn-glycerol-3-phosphate acyltransferase reaction. *Biochemistry* 38:5764–5771.
- Lu YJ, Zhang F, Grimes KD, Lee RE, Rock CO. 2007. Topology and active site of PIsY: the bacterial acylphosphate:glycerol-3-phosphate acyltransferase. *J. Biol. Chem.* 282:11339–11346.
- Machata S, et al. 2008. Lipoproteins of *Listeria monocytogenes* are critical for virulence and TLR2-mediated immune activation. *J. Immunol.* 181:2028–2035.
- Manoil C, Beckwith J. 1986. A genetic approach to analyzing membrane protein topology. *Science* 233:1403–1408.
- Munoa FJ, Miller KW, Beers R, Graham M, Wu HC. 1991. Membrane topology of *Escherichia coli* prolipoprotein signal peptidase (signal peptidase II). *J. Biol. Chem.* 266:17667–17672.
- Nilsson J, Persson B, von Heijne G. 2000. Consensus predictions of membrane protein topology. *FEBS Lett.* 486:267–269.
- Okugawa S, et al. 2012. Lipoprotein biosynthesis by prolipoprotein diacylglycerol transferase is required for efficient spore germination and full virulence of *Bacillus anthracis*. *Mol. Microbiol.* 83:96–109.
- Onufryk C, Crouch ML, Fang FC, Gross CA. 2005. Characterization of six lipoproteins in the sigmaE regulon. *J. Bacteriol.* 187:4552–4561.
- Paradis-Bleau C, et al. 2010. Lipoprotein cofactors located in the outer membrane activate bacterial cell wall polymerases. *Cell* 143:1110–1120.
- Pugsley AP, Cole ST. 1987. An unmodified form of the ColE2 lysis protein, an envelope lipoprotein, retains reduced ability to promote colicin E2 release and lysis of producing cells. *J. Gen. Microbiol.* 133:2411–2420.
- Qi HY, Sankaran K, Gan K, Wu HC. 1995. Structure-function relationship of bacterial prolipoprotein diacylglycerol transferase: functionally significant conserved regions. *J. Bacteriol.* 177:6820–6824.
- Robichon C, Vidal-Ingigliardi D, Pugsley AP. 2005. Depletion of apolipoprotein N-acyltransferase causes mislocalization of outer membrane lipoproteins in *Escherichia coli*. *J. Biol. Chem.* 280:974–983.
- Rost B, Sander C. 1994. Combining evolutionary information and neural networks to predict protein secondary structure. *Proteins* 19:55–72.
- Sankaran K, et al. 1997. Roles of histidine-103 and tyrosine-235 in the function of the prelipoprotein diacylglycerol transferase of *Escherichia coli*. *J. Bacteriol.* 179:2944–2948.
- Sankaran K, Gupta SD, Wu HC. 1995. Modification of bacterial lipoproteins. *Methods Enzymol.* 250:683–697.
- Sankaran K, Wu HC. 1994. Lipid modification of bacterial prolipoprotein. Transfer of diacylglycerol moiety from phosphatidylglycerol. *J. Biol. Chem.* 269:19701–19706.

49. Selvan AT, Sankaran K. 2008. Localization and characterization of pro-lipoprotein diacylglyceryl transferase (Lgt) critical in bacterial lipoprotein biosynthesis. *Biochimie* 90:1647–1655.
50. Serebryakova MV, et al. 2011. The acylation state of surface lipoproteins of mollicute *Acholeplasma laidlawii*. *J. Biol. Chem.* 286:22769–22776.
51. Shaner NC, et al. 2004. Improved monomeric red, orange and yellow fluorescent proteins derived from *Discosoma* sp. red fluorescent protein. *Nat. Biotechnol.* 22:1567–1572.
52. Sugai M, Wu HC. 1992. Export of the outer membrane lipoprotein is defective in *secD*, *secE*, and *secF* mutants of *Escherichia coli*. *J. Bacteriol.* 174:2511–2516.
53. Thompson BJ, et al. 2010. Investigating lipoprotein biogenesis and function in the model Gram-positive bacterium *Streptomyces coelicolor*. *Mol. Microbiol.* 77:943–957.
54. Tokunaga M, Loranger JM, Wu HC. 1984. Prolipoprotein modification and processing enzymes in *Escherichia coli*. *J. Biol. Chem.* 259:3825–3830.
55. Traxler B, Boyd D, Beckwith J. 1993. The topological analysis of integral cytoplasmic membrane proteins. *J. Membr. Biol.* 132:1–11.
56. Tschumi A, et al. 2009. Identification of apolipoprotein N-acyltransferase (Lnt) in Mycobacteria. *J. Biol. Chem.* 284:27146–27156.
57. Tusnady GE, Simon I. 2001. The HMMTOP transmembrane topology prediction server. *Bioinformatics* 17:849–850.
58. Typas A, et al. 2010. Regulation of peptidoglycan synthesis by outer-membrane proteins. *Cell* 143:1097–1109.
59. Urban S. 2010. Taking the plunge: integrating structural, enzymatic and computational insights into a unified model for membrane-immersed rhomboid proteolysis. *Biochem. J.* 425:501–512.
60. Vidal-Ingigliardi D, Lewenza S, Buddelmeijer N. 2007. Identification of essential residues in apolipoprotein N-acyltransferase, a member of the CN hydrolase family. *J. Bacteriol.* 189:4456–4464.
61. Viklund H, Elofsson A. 2008. OCTOPUS: improving topology prediction by two-track ANN-based preference scores and an extended topological grammar. *Bioinformatics* 24:1662–1668.
62. Wang Y, Zhang Y, Ha Y. 2006. Crystal structure of a rhomboid family intramembrane protease. *Nature* 444:179–180.
63. Widdick DA, et al. 2011. Dissecting the complete lipoprotein biogenesis pathway in *Streptomyces scabies*. *Mol. Microbiol.* 80:1395–1412.
64. Williams MG, Fortson M, Dykstra CC, Jensen P, Kushner SR. 1989. Identification and genetic mapping of the structural gene for an essential *Escherichia coli* membrane protein. *J. Bacteriol.* 171:565–568.
65. Wu Z, et al. 2006. Structural analysis of a rhomboid family intramembrane protease reveals a gating mechanism for substrate entry. *Nat. Struct. Mol. Biol.* 13:1084–1091.